FORUM GEOGRAFI
ISSN: 0852-0682 | E-ISSN: 2460-3945
HTTPS://JOURNALS.UMS.AC.ID/INDEX.PHP/FG/

Research article

Dams Overtopping Scenarios from Catastrophic Landslides in Mountains' Headwaters: Case Study in Kobe City, Japan

Christopher Gomez*

Faculty of Maritime Sciences, Kobe University, Kobe 658-0022, Japan

*) Correspondence: k0128086@gsuite.kobe-u.ac.jp

Citation:
Gomez, C., (2024). Dams overtopping scenarios from catastrophic landslides in mountains' headwaters: case study in Kobe City, Japan. Forum Geografi. 38(1), 1-10.

Article history:
Received: 21 January 2024
Revised: 11 March 2024
Accepted: 11 March 2024
Published: 17 March 2024

Abstract

As a Mw 8.0 Nankai Trough Earthquake is predicted with an 80% probability of occurrence within the next 30 years, the efficiency of check dams in the mountains above Kobe City is a crucial question when considering co-seismic landslide disaster risk management. In the present contribution, the author aimed to define which subsection of the Sumiyoshigawa watershed may be more prone to generate impacts downstream of Kobe City from catastrophic landslides in the headwaters. For this purpose, the present state of the check dams network was analysed from the 2018 LiDAR (Light Detection and Ranging) data, considering the progressive infilling of the structures. As a result, the capacity of the dams in 2018 dropped by about 1/10 of the original designed capacity, arguably because of the heavy rainfall events in 2014 and 2018. Despite this evolution, landslides > 20,000 m^3 starting from only one tributary can fill all the dams and flow downstream. This data makes it possible to prioritise dam curation programs, especially because population ageing and shrinking are reducing the manpower and the funds available to maintain the check dams.

Keywords: LiDAR; Landslides; SABO dams; Long-term Sedimentation.

1. Introduction

In Japan, a narrow coastal plain separating the sea and steep mountain or volcanic slopes - which occupy 70% of the land surface - has resulted in the need to control sediment hazards originating from the mountains (Siccard *et al.*, 2022) using check open and closed-dams made of steel frame, slit, culvert and steel and concrete dams (Dumont *et al.*, 2023). These structures are mainly designed to mitigate debris flows, which are concentrated mixtures of debris and water-flowing downslopes (Hungr et al., 2001). These events are triggered mainly by typhoons, heavy rainfalls (e.g., Guzzetti *et al.*, 2008), under the influence of earthquakes (Lin *et al.*, 2004), which in combination with heavy rainfalls can eventually lead to exceptionally long runouts (Gomez and Hotta, 2021).

The design of check dams (named Sabo dams when they were constructed by the Japanese Ministry of Land, Infrastructure, Transport, and Tourism) is also developed at the system level, notably using simulations such as the CASFPS or "Computer-Aided Sabo Facilities Planning System" (Mizuyama *et al.*, 1998), in which sediment fluxes are routed along the talwegs including the effects of filled and empty check dams, in order to assess hazard levels. Such an approach is particularly important, as check dams in typhoon-battered regions can fill up within a few years (Chiu *et al.*, 2021), and, under recurrent impacts, can become unstable (Liu *et al.*, 2022) and collapse (Zhang *et al.*, 2023) highlighting the importance of the network approach.

A check-dam system has been notably developed in the hills above Kobe City (Figure 1) because landslide and debris flow have been a common occurrence historically (Sokobiki *et al.*, 1996). As the Kansai Region (where Kobe City is located) is geographically close to the early power centre in Nara-city, there are records of hazards as early as year 799 referring to extensive floods (Table 1). Flooding from heavy rainfalls and typhoons have also been differentiated as early as 1728, showing an acute understanding of meteorological phenomena. Besides flooding, which dominates the record, references to what could be a landslide that blocked a road as early as year 836 are more clearly described in 1659, with the burial of temples in soil and mud. There is also, in 1820, the clear description of a landslide dam (Table 1), in the mountains above Kobe. Out of this record, at least two historical earthquakes were recorded, one in 1854 and a second in 1995: The Hyogo-Nanbu earthquake, which made Kobe City infamous (e.g. Yamaguchi and Yamazaki, 2001).

In this long record of environmental hazards, the 1995 Hyogo-Nanbu Earthquake stands out as the worst disaster in the region, with important building damages and loss of lives (e.g., Yamaguchi and Yamazaki, 2001). It has been depicted in great detail in terms of geophysical phenomena (Guo *et al.*, 2013) and hazard and disaster risk management (Shaw, 2013; Hashemi, 2015). In the hills of Mt. Maya and Mt. Rokko to the North of Kobe City, the earthquake triggered 2,615 landslides, of which 1,900 were directly connected to the stream network, and 715 were isolated in

the mountains (Table 2). Landslides mobilized a total volume of 746,720 m^3 in 1995, representing 236,720 m^2 that were impacted by erosion and deposition (Table 2).

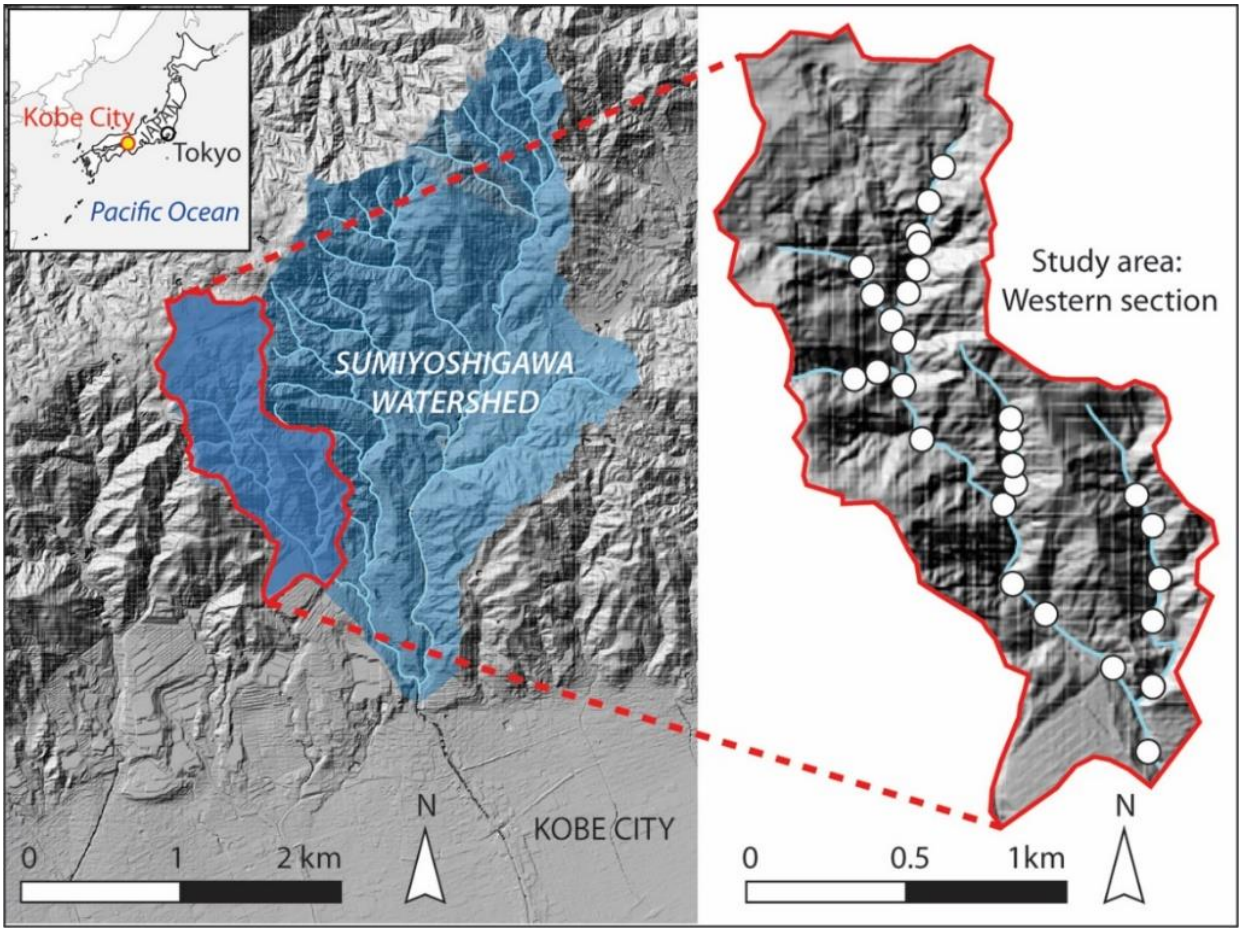

Figure 1. Location map of the Sumiyoshigawa Watershed North of Kobe City, and the western section used as the study area. The white dots represent each a check dam on the river network.

Table 1. Recorded natural hazards in today's Kobe City and the surrounding region, coded in dark blue: typhoon, in light blue: other floods, in yellow: earthquakes; in orange: sediment hazards and in white coastal floods (source: adapted and completed from the Sabo Office in Kobe, personal communication).

Year	Hazard reported	Year	Hazard reported
9/4/799	Extensive flooding	11/7/1860	Coastal storm and strong winds damage stone walls;
18/5/836	Some natural event blocked a road (landslide?)	15/8/1865	Levee breach of the Minatogawa River (7 death), levee breach of the Tennogawa River;
13/8/988	Large-scale flooding	7/1866	Levee breach of the Tennogawa River;
8/7/1302	Flooding	16/8/1866	Typhoon related flooding;
9/8/1475	Amagasaki-City, Hyogo City, Ashiya City experienced flooding	11/1868	Levee breach of the Tennogawa River
9/7/1544	Large scale flooding	18/9/1870	Severe winds and heavy rain cause various damages
6/8/1557	Large scale flooding	13/7/1873	Flooding in Kobe due to typhoon rainfall,
1608	February and August: flooding	2-3/10/1873	Levee breach of the Ikuta River due to heavy rainfalls
6/1614	Flooding in Kinai area	28/7-3/8/1874	Ikuta River and Minatogawa River levee breach due to heavy rainfalls
6/1637	Heavy-rainfall flooding in Hyogo area	16-18/5/1877	Extensive flooding through Kobe City
22/5/1659	Great flooding and "temples were buried in soil and mud".	6/1896	Continuous heavy rainfalls;
11/4/1674	Flooding in Kinai area	30/9/1896	Minatogawa break its banks;

Table 1. Recorded natural hazards in today's Kobe City and the surrounding region, coded in dark blue: typhoon, in light blue: other floods, in yellow: earthquakes; in orange: sediment hazards and in white coastal floods (source: adapted and completed from the Sabo Office in Kobe, personal communication) (Continued).

Year	Hazard reported	Year	Hazard reported
8/5/1676	Flooding in Kinai area	7-9/7/1903	Uji-River embankment damaged, 4 dead (heavy rainfall?);
6/1706	Great waves reported to have eroded the coast (tsunami?)	26/8/1905	Heavy rainfall (73.3 mm/h & 39 mm/20min)、10,000 dwellings flooded;
2/7/1712	Large river flooding along the Ikuta river (Kobe)	6-8/9/1910	251.8mm of rainfall triggered "The Big Flood";
8/7/1728	Flooding due to typhoon-triggered heavy rainfall	23/9/1912	Large typhoon from Shikoku to Osaka and total rainfall 159.7mm lead to extensive flooding;
1740	Ikuta River great flooding	11-12/9/1924	Typhoon (10 death and 1495 buildings flooded);
3/6/1742	Typhoon rainfall triggered: Gomao Village levee breach and flood; landslides in mountains	21/9/1934	Typhoon (precipitation: 26.5mm/h), 6 depth, 7919 buildings flooded to floor level; 2547 buildings flooded above floor level;
1754	Myohoji River levee breach	3-5/7/1938	Flooding(precipitation: day 1:49.6mm, day 2:141.8mm, day 3:270.4 mm): 1497 houses washed off; 966 submerged; 2658 destroyed; 7878 partially destroyed; 31,643 houses partially flooded; 75,252 houses flooded to floor level; 671 deaths, 24 missing; 14 embankment breaches; 69 roads washed away, 57 bridges lost;
29/5/1756	Ikuta River flooding and inundation of buildings	1/8/1939	Heavy rainfall (87.7mm/h), 14,165 buildings flooded, 2 deaths、23 embankments breaches;
27/5/1768	Extended flooding	8-11/10/1945	Typhoon with 49.6 mm/h), led to 87 embankments breaches, 141 roads damaged and 61 bridges washed away;
6/1774	Tsunami	18-19/6/1946	Heavy rainfalls led to 53 river breaches, 46 roads damaged and 12 bridges lost
12/6/1779	Flooding of the Kinai Region due to typhoon	3/7/1947	Flooding led to 3 houses submerged, 7 half flooded, 2 wahsed away, 228 flooded above floor level and 5862 houses flooded up to floor level;
23/7/1779	Flooding of the Kinai Region	21/7/1948	Flooding led to 8 deaths, 10 houses evacuated, 26 houses destroyed, 1077 flooded above floor level and 2,425 flooded below floor level;
12/8/1785	Flooding of the Kinai Region	18-19/6/1949	Typhoon led to the transport and accumulation of 21,778m^3 of sediments (most likely landslides and/or debris flows)
4/1791	Waves (tsunami?) entering the village of Wakihama	3/9/1950	Typhoon with 161mm of rain led to 1067 houses destroyed, 39 washed away, 58 flooded above floor level, 2682 flooded above floor level, 44 embankment breaches, 70 roads damaged;
25/7/1800	Flooding of Minatogawa (today in Kobe City) and assignment of 500 laborers to water defenses	6/7/1953	Typhoon nb 2 took the lives of 2, flooded 673 houses, damaged 30 roads and breached embankments at 37 locations;
6/1815	Flooding of the Kinai region	5/9/1953	Typhoon 13 destroyed 689 houses, flooded 1047;
3/8/1816	Extensive flooding of the Kinai region	24-27/6/1961	Rainfall 472.1 mm: 28 dead and 3 missing; 140 houses were destroyed, 263 houses were partially destroyed, 3960 houses were flooded above flood level and 29,376 below floor level; riverbank damages occurred at 973 locations and 580 roads were damaged and 62 bridges washed away;
23/5/1820	Collapse of the Tenjin Mountain in Nagata (Kobe) and creation of the Namekura landslide dam ponding.	16/9/1961	Heavy rainfall: killed 10, washed away 2,555 houses, flooded above floor level 8,801 and 36,034 below floor level, damaging river embankments in 98 locations with various river impacts in 1,756 locations; a total of 1,044 road damages were recorded and 121 bridges damaged;
8/4/1821	Large scale flooding of the Kinai region	10/9/1965	Typhoon 23 (118.6 mm rain) led to 1,756 houses being destroyed, 2,603 flooded above floor level and 1,262 below floor level;
26/4/1829	Minatogawa at levees height, mobilization of people against the flood	9/7/1967	Heavy rainfall (total 317.7 mm over 4 days, with maximum 75.8 mm/h) killed 90 + 8 missing, destroyed 367 houses, damaged 390 and flooded above floor level 9,187, and 49,650 below floor level. It triggered 141 landslides, 168 rockslides and river flooded in 74 locations.

Table 1. Recorded natural hazards in today's Kobe City and the surrounding region, coded in dark blue: typhoon, in light blue: other floods, in yellow: earthquakes; in orange: sediment hazards and in white coastal floods (source: adapted and completed from the Sabo Office in Kobe, personal communication) (Continued).

Year	Hazard reported	Year	Hazard reported
19/3/1843	Flooding of the Minatogawa River "beyond expectations".	17/1/1995	Hanshin-Awaji "daishinsai" (Hyogo-Nanbu earthquake): at 5:46 a Mw 7.3 earthquake took the lives of 6,402 individuals, 104,004 buildings were destroyed, another 136,952 were heavily damaged, 7,035 were burnt down by fire; 89 partially burned.
4/11/1854	Large-scale earthquake in the morning;	5-8/7/2018	Heavy rainfall (506.5 mm) with 9 locations above 400 mm in Hyogo Prefecture led to 2 deaths and 12 missing, as well as 140 buildings damaged and 781 flooded to different levels, it resulted in 31 important landslides and rockfalls;
6-22/51857 7/1857	Uninterrupted of rainfall; Flooding in the Kinai area;	3-5/9/2018	Typhoon with winds up to 46.5 m/s and storm surge of 2.3 m in Kobe City led to 11 deaths, 694 injured and extensive flooding;

Table 2. Landslides and sediment volumes were displaced four years following the Hanshin-Kobe earthquake (data courtesy of the Kobe Sabo office).

Surface		Landslide units		Landslide	Volume of Sediments	
	Year	[Nb]	[Nb/km^2]	Surface [m^2]	[m^3]	[m^3/km^2]
120 km^2	1995	2,553	15.9	263,720	746,720	5,040
	1996	97	0.6	2,000	2,010	20
	1997	31	0.2	1,012	2,879	20
	1998	23	0.2	1,689	2,170	10
	1999	111	0.7	9,483	17,615	120

From these premises, two elements motivated the research questions: (1) nearly 30 years after this catastrophic earthquake in Kobe, a number of the check dams must have been partially or fully filled (notably after the heavy rainfall event of 2018, for instance, cf. Figure 2); (2) as the Nankai Trough Earthquake is predicted to occur with a probability of 80% in the next coming 30 years, co-seismic landslides are likely to occur, and if the earthquake was not to occur during the cold and dry season but during the Spring to Autumn wet season, then the size of landslides may be much larger. In light of this issue, this paper aims to (1) find the level of infilling of the check dams in the West-section of the Sumiyoshigawa basin and (2) simulate how the network of check dams in its present state would react to different landslide scenarios in different portions of the watershed.

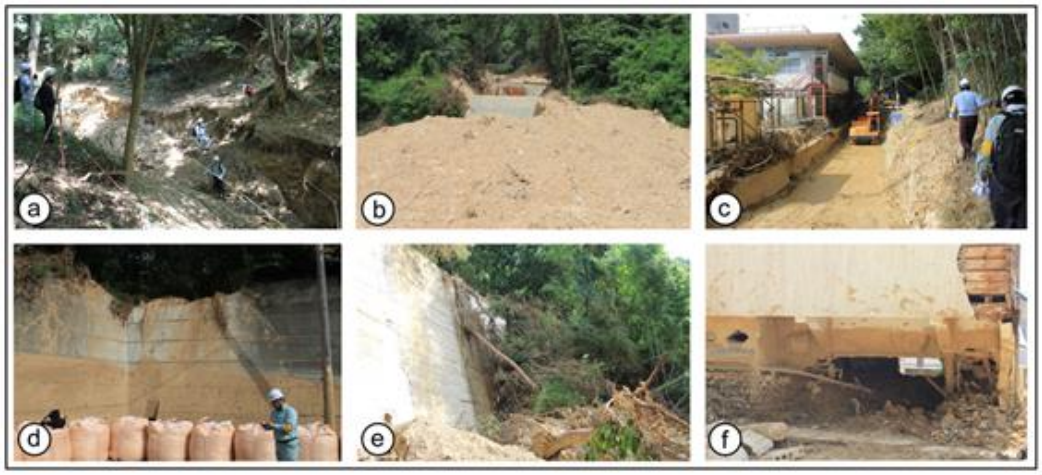

Figure 2. Photographs of the 2018 heavy rainfall event that triggered (a) erosion in the hills, (b) destroyed a check dam in the Sumiyoshigawa River, (c) eventually flowing down to the dwellings of Kobe City by (d) overtopping protection walls and (e) check dams, eventually filling houses with sediments, blocks, and driftwood (f).

2. Research Methods

The Sumiyoshigawa (Sumiyoshi meaning old living area and gawa (or kawa) meaning river) has 71 check dams, 66 being closed dams, 4 with openings with a slit grid, and 1 being a slit dam. For the present contribution, the author investigated a watershed section, often referred as the West section, in opposition to the main river (Otani). The studied section comprises 28 dams distributed on a channel network with three small true-right tributaries and one longer tributary on the true left side (Figure 3).

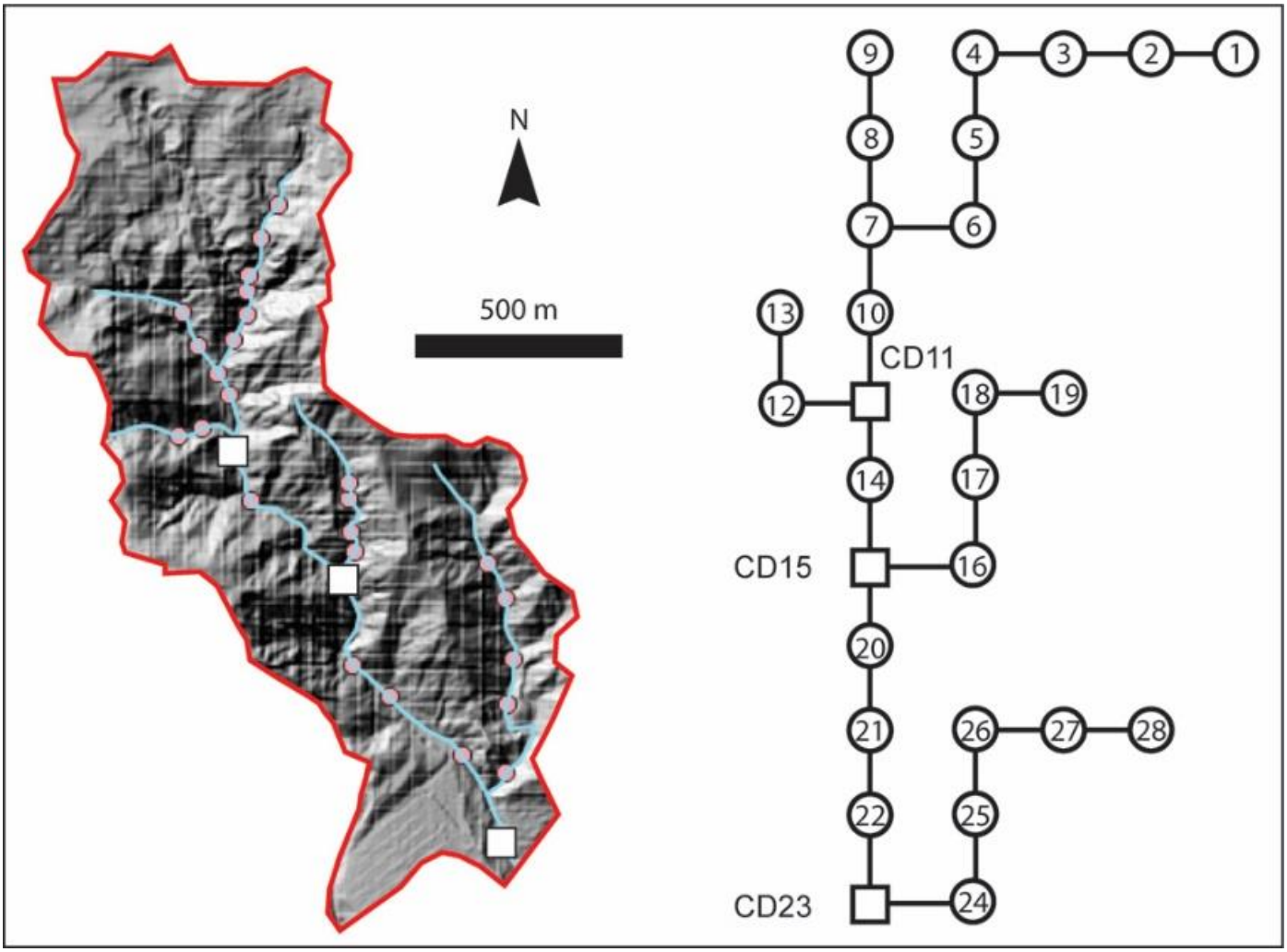

Figure 3. Network of dams used in the simulation, with the dams 11, 15, and 23 being the controlled dams from which the results are presented. They are "key-indicator" nodes in the network, showing the influence of different parts of the network on the sediment transfer.

2.1 Material

The topography used to delineate the watershed, find the check dams, and determine their present infilling level was generated from the 2016 LiDAR dataset flown over the Kobe area on July 11th. The LiDAR used in the present survey is a Trimble Harrier56, which generated points at 180 kHz, with a scanning swath occurring at 49 Hz per swath. The LiDAR was mounted on a Robin R44II helicopter, which travelled at 20 m/s. It resulted in a LiDAR point cloud of 10 points/m^2. The LiDAR data was spatialized using the internal IMU, the onboard GNSS, and three GNSS stations spread around the survey area. Furthermore, 10 locations visible from the sky calibrated the point cloud. The Root Mean Square Error between the GNSS points and the LiDAR was on average 0.05 m with a maximum value of 0.07 m.

2.2 Data Processing

The LiDAR data was imported in CloudCompare®, and as true 3D data was not necessary, the ground level was converted to a topographic grid with a 1 m horizontal resolution. Then, using the open-source GIS software QGIS, the height of the dams, the surface of the sediment trapped in the dam, and the calculation of the capacity of each dam were performed using the profiler add-

on and the standard geometric tool associated with shapefiles. The GIS data generated a network of dams, including their capacity in 2018.

2.3 The network model

The network was programmed in Python using the standard Numpy library. Each dam was created as an object, and each dam object was associated with a set of attributes (capacity, level, upstream and downstream slopes, distances, and inflow and outflow). This structure was chosen to develop the model further and have a set of objects to redeploy over different configurations.

Over this network, inputs of sediments are added to the headwater and then routed through the system. In the present contribution, a simple marching algorithm was implemented as the result was to see the results at the exit of the network.

The input of sediments was divided into scenarios with landslides ranging from 1,000 m^3 to 20,000 m^3. As this contribution focuses on landslides in headwaters, six triggering locations were chosen, and at each location, 15 sub-scenarios were run successively. The choice of scenario was based on the observations of sediment transfer volumes reported during the Hyogo-Nanbu earthquake (Figure 2) and the possibility of a catastrophic landslide that would exceed the precedent values like it has been observed in extreme cases (e.g., Shiaorin landslide in Taiwan). As the headwater surfaces above dams 2, 3, 9, 13, 19, and 28 are respectively 0.144 km^2, 0.153 km^2, 0.138 km^2, 0.046 km^2, 0.1 km^2, and 0.04 km^2, single landslides are not expected to exceed 800 m^3 on average based on the previous earthquake data. However, the 1995 earthquake occurred in January, a dry season in Kobe. If the same event were to occur between May and November, the event would certainly change in magnitude. To consider potential underestimation due to the season, the present contribution tests scenario from 1,000 m^3 to 20,000 m^3, which can be compared to 1 m thick shallow landslides impacting between 20% and 40% of the headwater surface. Finally, the discrete results from the models linking landslides' volumes (x in eq. 1) to the different dams' infilling levels y was written in a continuous format using logistic models (Equation 1). where L is the limiting value (maximum value), and k represents the rate of change towards the maximum L value.

$$f(x) = \frac{L}{1 + \epsilon^{-k(x-x_0)}} \quad (1)$$

3. Results and Discussion

3.1. Dam infilling levels in 2018

The free volume of each of the 28 dams was calculated to be, on average, 1749 m^3, with a minimum of 0 m^3 (check dam full) to 8050 m^3., and a total volume retainable in the network of 49,000 m^3 in 2018. These volumes are only a fraction of the originally designed retention volumes (Figure 4). For the dams of which the original designed volume was available, the smallest dams with originally 10,000 m^3 only have between 950 m^3 and < 8,000 m^3 remaining. Larger dams have also shown a similar trend (Figure 4). This shows that the dams were initially well-calibrated to their environment, but the threat due to dam overtopping needs reassessment.

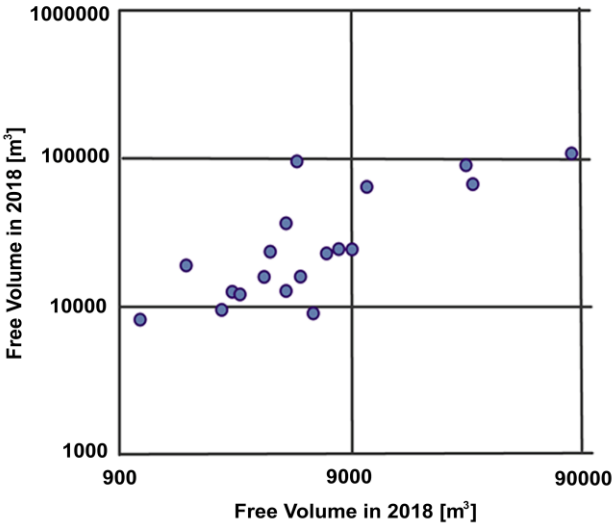

Figure 4. Comparison of the free volume in 2018 with the original designed volume.

However, the infilling levels and the original design are not following a linear correlation and some dams have filled faster than others. This discrepancy is set to impact the location of landslides in the watershed. For landslides triggered at dams 2 or 3 in the headwaters, landslides up to 20,000 m^3 are not expected to translate sediments in the lower areas of the watershed (Figure 5).

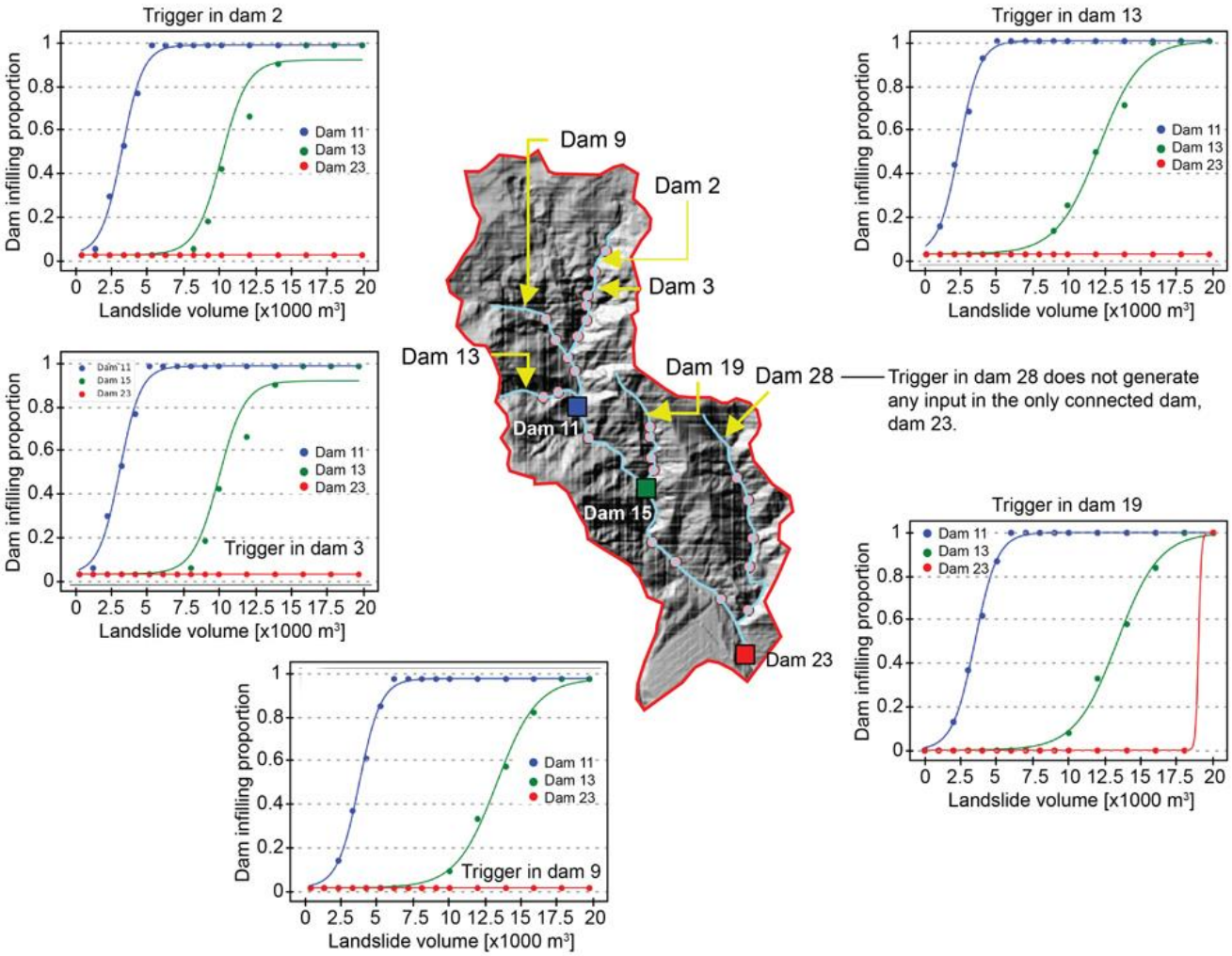

Figure 5. Reaction of the network at three control nodes (dams 11, 15 and 23) to the input of a landslide in each branch of the channel network (dams 2, 3, 9, 13, 19 and 28).

Control dam 11 is filled for landslide volumes > 2,500 m^3 to 5,000 m^3, while control dam 15 is filled if the landslide > 12,000 m^3. If dam 11 reaches 100% infilling. The half mark is reached for a landslide between 2,000 and 3,000 m^3 at dam 11, while it takes a landslide of 10,000 m^3 to 12,500 m^3 to infill dam 15 (Figure 5). Triggers from any of the two short tributaries (in dam 3 and dam 9) show a similar pattern with a rapid infilling of dam 11, while dam 15 needs a landslide >18,000 m^3 to be filled. From these two last scenarios, dam 23 downstream is unaffected. Only the scenario with a landslide starting in dam 19 with >20,000 m^3 shows sediments that can travel past dam 23 (Figure 5).

Systematically comparing the scenarios that would start in the main section of the channel against the tributaries, it appears that the tributaries are eventually posing the highest risk (Figure 6) when starting from dam 9 or 13, as dams 11 and 15 are infilling faster. However, when comparing landslides triggered in the main stem (dam 2) against the tributary of dam 19, a slight lag in the opposite direction can be observed, and dam 15 is infilling for slightly smaller when the landslide is triggered in the main stem. Compared to these single landslide scenarios, however, if two landslides of the same size were to occur in two tributaries (for instance, tributary 9 and 13), all three control dams would infill for landslides <14,000 m^3 each. If one single landslide > 20,000 m^3 triggered above dam 19 can generate a flux of sediment at the exit of the research basin, it takes a combined total of 25,000 m^3 from the tributaries 9 and 13 for a flow to pass dam 23 (Figure 6).

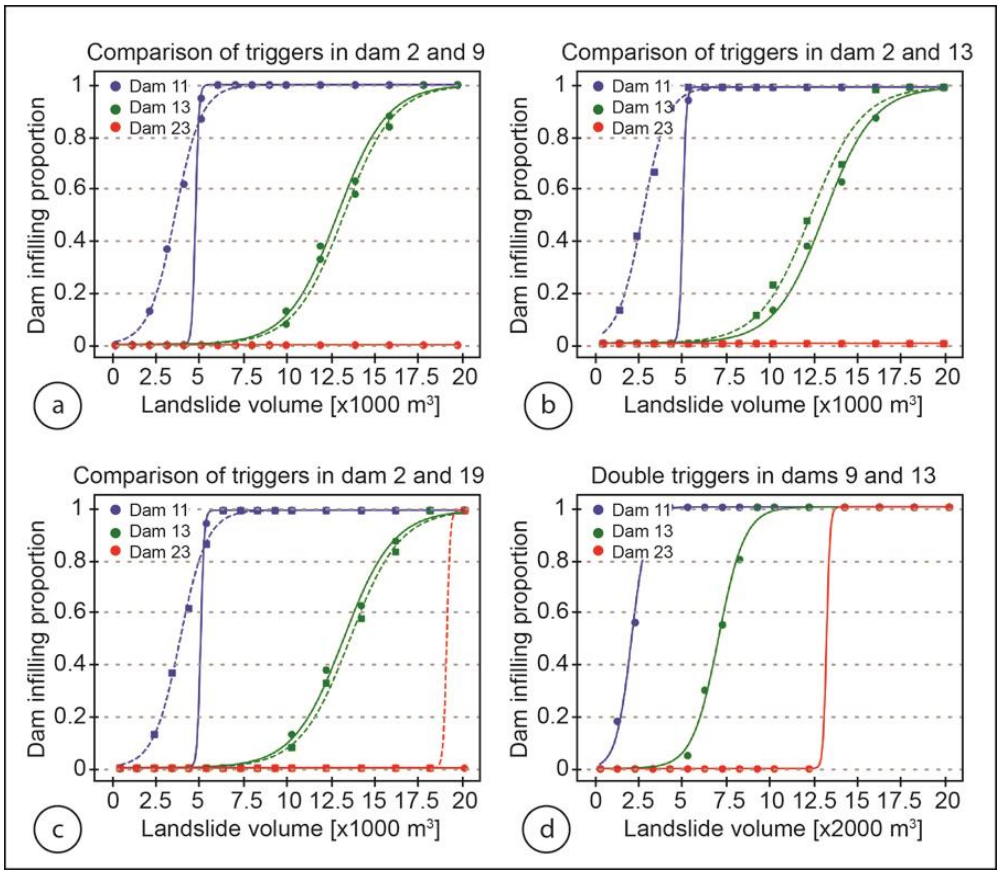

Figure 6. Comparison of the scenarios from the tributaries against scenarios from the main channel, as well as a scenario with two landslides together. The dotted lines represent the tributaries in (a, b,c), i.e. a landslide triggered in dam 9, 13, and 19.

3.2. Discussion

From the present analysis, the network of check dams in the Western section of the Sumiyoshigawa is a safe network that can capture sediments potentially produced in the headwaters by any landslide < 20,000 m^3 (please note that it assumes no dam collapse), except if the landslide occurs above dam 19. In such a case, sediments can flow downstream to dam 23. In any other case, two concomitant landslides are needed for sediment to overcome dam 23, with a combined volume of at least 25,000 m^3 of material from dams 9 and 13.

From the result of the present analysis, marginal weaknesses can be highlighted. However, the existing network approach in designing check dams (Mizuyama *et al.*, 1998) provides reliable protection to landslides up to 20,000 m^3, even several decades after the construction of the structures (Figure 7). This adequacy of the system is further demonstrated by the infilling rate of the check dams, which is grossly correlated with the originally designed volume following a relation y=0.0017x + 122.75, with a R2 of 0.76 (Figure 7).

However, in comparison to punctual events, such as co-seismic landslides, one question that arises is the role of background erosion and how it impacts the network over long periods, especially because climate change is set to trigger more intense rainfall events and typhoons over the Japanese archipelago and East Asia (Chiang and Chang, 2011, Saito *et al.*, 2014; Wang, 2013), which in consequence will result in an acceleration of dam infilling, mainly because the soil of the Sumiyoshigawa catchment is a deep altered granite, which is unlikely to result in a sediment production limited regime. Using a set of erosion plots in the mountains between 250 m and 490 m a.s.l., with slope inclination of 15, 23, 30 and 31 degrees, recorded erosion ranged between 0.1 g/m^2/month to < 800 g/m^2/month, with the maximum being isolated peaks (Figure 8). During the period 2003 to 2006, when plot erosion surveys were conducted, an average monthly erosion of 105 g/m^2/month was measured at plot number 2, which is denuded. Under vegetation cover, the erosion was recorded at the three other locations as 5.7 g/m^2/month, 7.4 g/m^2/month, and 0.3 g/m^2/month. In light of these results, and considering a material density of 2.1 to 2.5 g/cm^3, it is safe to rule out the progressive accumulation of sediments from background erosion as a threat to the safety and usability of check dams.

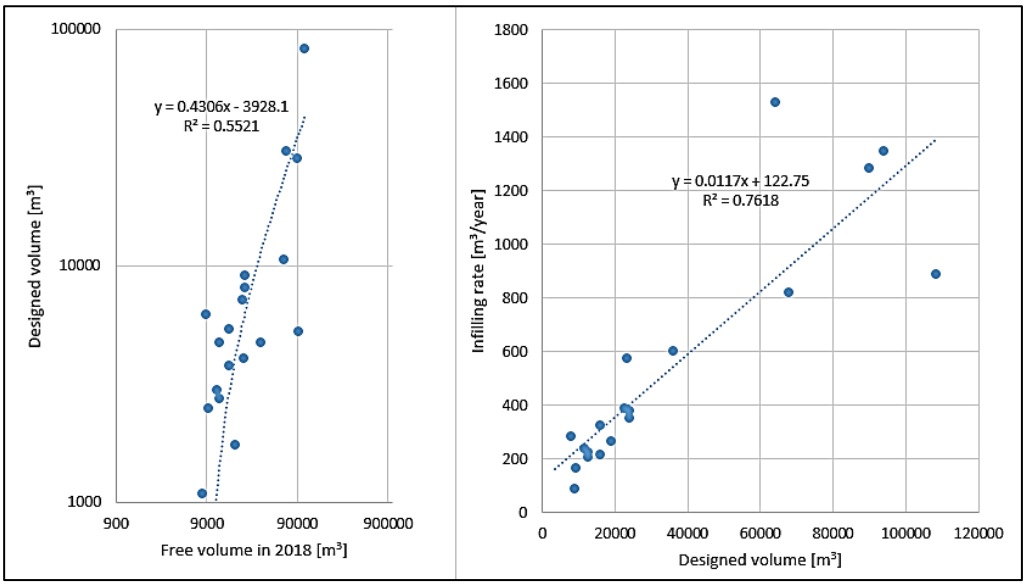

Figure 7. Correlation between the free volume in 2018 and the originally designed volume, as well as the designed volume and the infilling rate for 19 dams, for which original data were available.

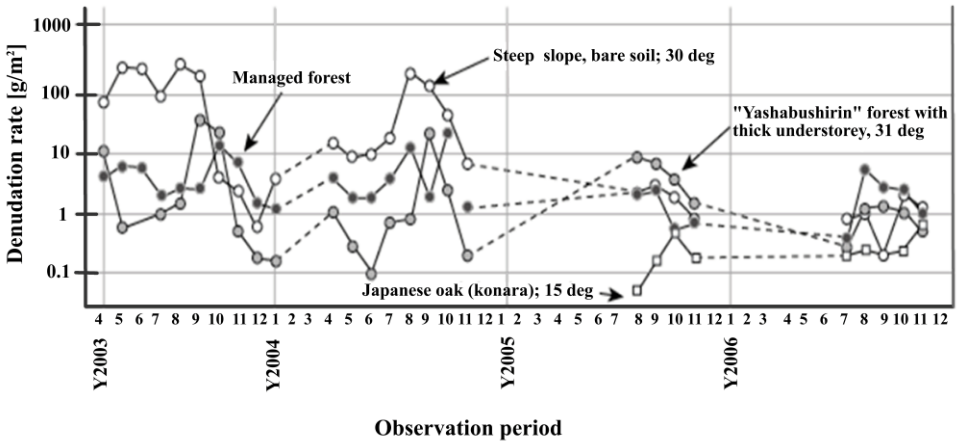

Figure 8. Background erosion of the slopes in managed forest, Japanese oak and in thick forest with slopes ranging from 15 to 31 degrees between 2003 and 2006, from measured forest plots.

4. Conclusion

Check dams deployed in the network are a strong hard-engineering measure to protect assets and population when relocation is impossible. Moreover, good dam calibration also shows that the network can have long-lasting positive impacts even with minimum maintenance. However, it is a safe system for average hazards and disaster risk and do not protect against larger events. It is a general problem that remains in disaster risk management, where the management of small and middle-sized events is the focus of these policies, but it also gives a false sense of security as it is ineffective against extreme events. In the midst of this work, I also realized that hydrologists and geomorphologists had been focusing their attention on natural systems in or-der to fathom their mechanisms. However, there are comparatively very few studies that look at the impacts of check dams on water and sediment transfers (e.g., Norman *et al.*, 2016; Yazdi, 2017), and how they influence the geometry as well as the evolution of the stream network, and in turn the generation of hazards such as landslides, and further work is necessary on this front as well.

Acknowledgements

This research was funded by the Hyogo Science and Technologi-cal Association Research Grant. The authors are also in debt to the Kobe Sabo Office and the Kobe City Of-fice for providing sets of hydrolog-ical and geo-morphological data.

Author Contributions

Conceptualization: Gomez, C.; **methodology:** Gomez, C.; **investigation:** Gomez, C.; **writing original draft preparation:** Gomez, C.; **writing review and editing:** Gomez, C.; **visualization:** Gomez, C. The author have read and agreed to the published version of the manuscript.

Conflict of interest

All authors declare that they have no conflicts of interest.

Data availability

Data is available upon Request.

Funding

This research received no external funding.

References

Chiang, S. H., & Chang, K. T. (2011). The potential impact of climate change on typhoon-triggered landslides in Taiwan, 2010-2099. *Geomorphology*, 133 (3-4), 143-151. doi: 10.1016/j.geomorph.2010.12.028.

Chiu, Y. F., Tfwala, S. S., Hsu, Y. H., Chiu, Y. Y., Lee, C. Y., & Chen, S. C. (2021). Upstream morphological effects of a sequential check dam adjustment process. *Earth Surface Processes and Landforms*, 46, 2527-2539. doi: 10.1002/esp.5178.

Dumont, M., Gomez, C., Arnaud-Fassetta, G., & Lissak, C., Viel, V. (2023). The Disaster Protection System of Mountainous Rivers in Japan: The Example of the Akatani Watershed's Reconstruction. *Sustainability*, 15(21), 15331, doi: 10.3390/su1521155331.

Gomez, C., Hotta, N. (2021). Deposits' Morphology of the 2018 Hokkaido Iburi-Tobu Earthquake Mass Move-ments from LiDAR & Aerial Photographs. *Remote Sensing*, 13(17), 3421. doi: 10.3390/rs13173421.

Guo, Y., Kobetsu, K,. & Ohno, T. (2013). Analysis of the rupture process of the 1995 Kobe earthquake using a 3D velocity structure. *Earth, Planets and Space*, 65, 1581-1586. doi:10.5047/eps.2013.07.006.

Guzzetti, F., Peruccacci, S., Rossi, M., & Stark, C.P. (2008). The rainfall intensity-duration control of shallow landslides and debris flows: an update. *Landslides*, 5, 3-17. doi: 10.1007/s10346-007-0112-1.

Hashemi, S. A. A., & Kashi, H. (2015). Determination of number of check dams by artificial neural networks in arid regions of Iran. *Water Science and Technology*, 76(6), 952-959. doi: 10.2166/wst.2015.268.

Lin, C. W., Shieh, C. L., Yuan, B. D., Shieh, Y. C., Liu, S. H., & Lee, S. Y. (2004). Impact of Chi-Chi earthquake on the occurrence of landslides and debris flows: example from the Chenyulan River watershed, Nantou, Taiwan. *Engineering Geology*, 71, 49-61. doi: 10.1016/S0013-7952(03)00125-X.

Liu, D., You, Y., Liu, J., Mu, Q., Feng, J., Zhang, L., Wei, A., & Tan, H. (2022). Stability analysis of check dam impacted by intermittent surge. *Bulletin of Engineering and the Environment*, 81 (53), 1-15. doi: 10.1007/s10064-021-02539-1.

Mizuyama, T., Tomita, Y., Ido, K., & Fujita, M. (1998). Computer-Aided Sabo facilities Planning System – A Case Study of the Sumiyohi River in the Rokko Mountains. *Sabougakkaishi* 50 (6), 40-43. doi: 10.21203/rs.3.rs-3753562/v1

Norman, L. M., Brinkerhoff, F., Gwilliam, E., Guertin, D. P., Callegary, J., Goodrich, D. C., Nagler, P. L., & Gray F. (2016). Hydrologic Response of Streams Restored with Check Dams in the Chiricahua Mountains, Arizona. *River Research and Applications*, 32, 519-527. doi: 10.1002/rra.2895.

Saito, H., Korup, O., Uchida, T., Hayashi, S., & Oguchi, T. (2014). Rainfall conditions, typhoon frequency, and contemporary landslide erosion in Japan. *Geology*, 42(11), 999-1002. doi: 10.1130/G35680.1.

Shaw, R. (2013). 'Kobe Earthquake: Turning Point of Community-Based Risk Reduction in Japan' in Shaw, R. *Community Practices for Disaster Risk Reduction*, 21-31. doi: 10.1007/978-4-431-54246-9.

Siccard, V., Lissak, C., & Gomez, C., (2022). From slope instabilities to sedimentary sources: study of the 5-6, 2017 geomorphic disaster in the Chikugo watershed (Kyushu, Japan). *Geomorphologie, Relief, Envi-ronnement et Processus*, 28 (4), 257-271. doi: 10.4000/geomorphologie.17395.

Sokobiki, H., Kobashi, S., Habara, T., (1996). Studies on the Debris-flow in Rokko District (Part 2). *Journal of the Japan Society of Engineering Geology*, 27 (3), 119-127. doi: 10.5110/jjseg.27.119.

Wang, G. Z., Mei, Y.D., Qu, J.G., Shuang, R., & Xu, J. (2013). Prediction of Siltation from a Rainfall in Check Dam Based on RBF Neural Network. *Applied Mechanics and Materials*, 263-266, 2150-2154. doi: 10.4028/www.scientific.net/AMM.263-266.2150.

Yamaguchi, N., & Yamazaki, F. (2001). Estimation of strong motion distribution in the 1995 Kobe earthquake based on building damage data. *Earthquake Engineering and Structural Dynamics*, 30 (6), 787-801. doi: 10.1002/eqe.33.

Yazdi, J. (2017). Check dam layout optimization on the stream network for flood mitigation: surrogate model-ling with uncertainty handling. *Hydrological Sciences Journal*, 62 (10), 1669-1682. doi: 10.1080/02626667.2017.1346376

Zhang, Q., Yanlong, L., Yu, S., Wang, L., Chen, Z., & Zhou, J. (2023). Rapid quantitative study of check dam breach floods under extreme rainstorm. *Natural Hazards*, 116, 2011-2031. doi: 10.1007/s11069-022-05751-8.